Towards an autonomous robotic platform for percutaneous procedures

Valentina Corbetta, Alice Segato, Andrea Fortuna, Tommaso Magni, Mattia Magro, Xiu Zhang and Elena De Momi

Department of Electronics, Information and Bioengineering, Politecnico di Milano

INTRODUCTION

Structural Intervention Cardiology (SIC) procedures still present limitations (e.g. use of fluoroscopy with consequent radiation exposure, lack of force or haptic feedback, risk of embolisation or perforation) [1]. The ARTERY proposes an autonomous robotic platform to overcome these drawbacks.

MATERIALS AND METHODS

A. Real environment: actuating the ARTERY catheter

The MitraClip (MC) system is composed of two catheters, the sheath catheter and the delivery catheter; the latter is inserted in the first. Therefore, we need two separate, yet similar, actuation systems, as depicted in Figure 1B.1 and Figure 1B.2. Studying how the components of the MC system are handled by the surgeon during procedures [2] led to choose a motorize stabilizer for actuation, as seen in Figure 1B. The two main elements for actuation are the following:

- Stepper motors (1.a, 2.b, 2.c) to grant the possibility of rotation for the whole system. They must able to generate a holding torque greater than 0.6 Nm;
- Linear actuators (1.b, 2.a) that convert the rotation of the motor's shaft into a translation movement, properly mimicking the displacements of the whole system.

These components are designed in Solidworks and printed in Polylactic acid (PLA) material via the S3 3D printer (Ultimaker). This design was properly connected to the MC system to obtain the first prototype of the experimental setup. The first attempt to control the MC is performed using an Arduino One, exploiting a joystick (Figure 1B.7): different buttons actuate different motors.

B. Virtual environment

Starting from a Computed Tomography (CT) scan (dimension $512 \times 512 \times 347$) provided by IRCCS Ospedale San Raffaele, we reconstructed in Unity the anatomical environment in which the agent (i. e. the catheter) moves. In 3D Slicer, the original scan has been manually segmented to obtain the anatomical structures of interest (i. e. right and left atria and ventricles, inferior and superior vena cava, femural veins, pulmonary artery) and subsequently smoothed, filtered with a gaussian filter. At last, it was hollowed in MeshMixer. The final result is shown in Figure 1A. The purpose of the simulation environment is to allow pre- and intra-operative path planning. To this end, we have created two different environments: pre-operative, which is static, and intra-operative, which is dynamic, as it simulates the pulsing of the heart and the vessels. We implemented a manual path planner controlled using a joystick. The surgeon can thus design and visualize all the possible trajectories in real time in the specif patient's anatomy and select the best one.

C. Bridging the real and virtual environments: Cosserat rod theory

To have an accurate representation of the real catheter in the virtual environment, it is paramount that the virtual catheter behaves as the real one in terms of geometry and kinematics. For this reason we have applied Cosserat rod theory to represent the MC geometry [3]. Cosserat rod theory employs a robot-attached reference frame composed by a matrix $\boldsymbol{R}$ (orientation) and a vector $\boldsymbol{p}$ (position). The robot configuration is evaluated in a fixed number of points, named nodes, placed along the rod. Solving the system for the nodes allows to obtain a reliable representation of the body. The frame is attached to the nodes and its evolution along the body length s is described by means of a system of differential equations:

$$\begin{aligned} \dot{R}(s) &= R(s)\hat{u}(s) \\ \dot{p}(s) &= R(s)v(s) \end{aligned} \tag{1}$$

To represent the rod geometry, we need to compute the values of angular u(s) and linear v(s) rate of change of each node. In order to find v and u, Cosserat rod theory uses equilibrium equations between internal and external moments and forces for each node:

$$\dot{\mathbf{n}}(s) + \mathbf{f}(s) = 0 \tag{2}$$

$$\dot{\mathbf{m}}(s) + \dot{\mathbf{p}}(s) \times \mathbf{n}(s) + \mathbf{l}(s) = 0$$

At last, the internal force and moment are related with v and u, exploiting constitutive material laws:

$$\begin{aligned} \mathbf{n}(s) &= R(s)K_{se}(s)(\mathbf{v}(s) - \mathbf{v}^*(s)) \\ \mathbf{m}(s) &= R(s)K_{bt}(s)(\mathbf{u}(s) - \mathbf{u}^*(s) \end{aligned} \tag{3}$$

Combining (1), (2), (3), we obtain the complete set of Cosserat rod model derivative equations to be solved.

Evaluating the system in the nodes gives a mechanics-based representation of the robot shape.

RESULTS

D. Real environment

In Table I are reported the specifications of the main components chosen for the experimental setup.

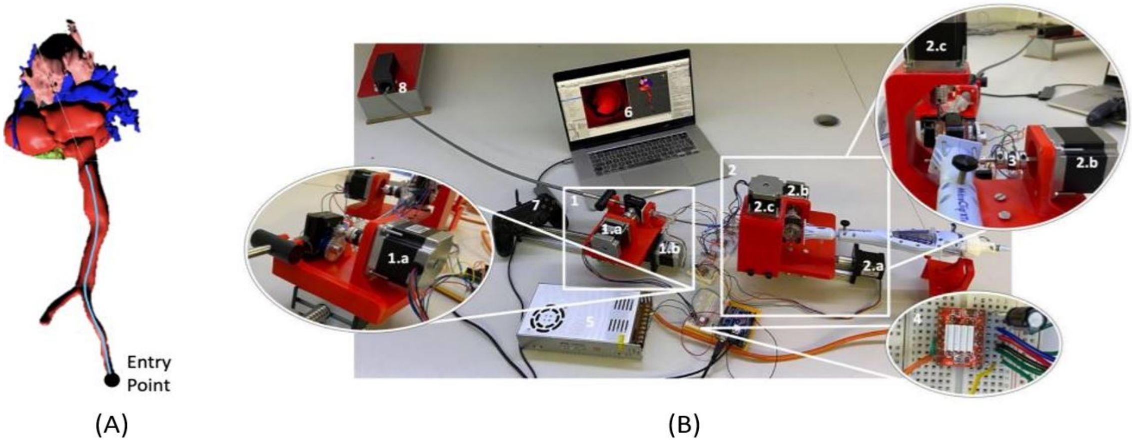

Fig. 1: *(A) 3D model of cardiovascular environment and path planning results (light blue path); (B) ARTERY set up. Two main structures: (1) sheath catheter's actuation and (2) delivery catheter's actuation. Motor (1.a) allows the rotation of the external guide (i.e. sheath catheter); linear actuator (1.b) permits its insertion; linear actuator (2.a) works on the insertion of the delivery catheter and on the best positioning of the clip, using motors (2.b) and (2.c). The shafts of the motors and of the catheter are connected through oldham adapters (3). A4988 driver (4) controls the motor through the Arduino One and (5) is the 24V power supply. (6) shows the virtual environment and (8) emulates the femural vein Entry Point.*

TABLE I: Experimental setup's components

Components	Number	Weight [kg]	Torque [Nm]
Nema 17 Stepper Motor	3	0.350	1.26
Oldham adapter	3	0.05	1.7
Linear Actuators	2	1.36	2

E. Virtual environment

The trajectories designed in the simulation environment are evaluated in terms of minimum and average distance kept from the delicate structures (e.g. wall of vessels) and time to reach the target. Table II reports the averaged results on 10 manually executed trajectories.

TABLE II: Trajectories' parameters

Results	Min Distance [mm]	Mean Distance [mm]	Time [s]
Value	2.74	3.99	47.0

Figure 2 shows the output of the kinematic model when the catheter is subject to the gravity force along the z-axis and the displacements of the tendons. In particular, the first tendon is subjected to a 2.5 cm displacement, accordingly the third one is released by the same amount, we don't have any displacement for the tendon on the top. The resulting position of the end effector is equal to
$p = [0.3, -0.33, 0.24]$.

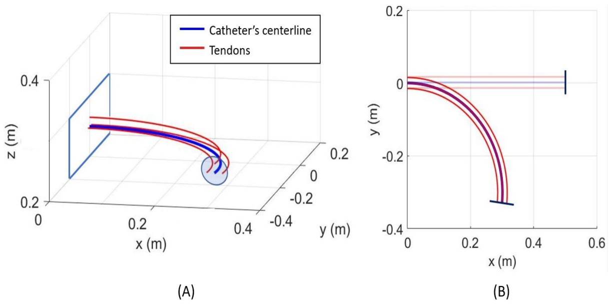

Fig. 2: *(A) Catheter's kinematic model with gravity force and tendons displacements; (B) The top view shows the deformation of the catheter with respect to the original position.*

CONCLUSIONS AND DISCUSSION

This works presents the first steps towards the the development of an autonomous robotic platform for percutaneous procedures, exploiting a digital twin approach. Indeed, the actuation of the physical catheter shows promising results, as we are now able to control the catheter via a joystick. The kinematic behaviour of the real catheter is well predicted by the kinematic model, that will be the basis of our final control strategy. Finally, our virtual environment allows us to find the best possible path in simulation. We will use the manual virtual planner to collect a series of demonstrations performed by surgeons that will be used to train a Deep Reinforcement Learning Model based on the principal of learning from demonstrations. Integrating all these components will lead towards an autonomous platform.

REFERENCES

[1] P. Legeza, G. W. Britz, T. Loh, and A. Lumsden, "Current utilization and future directions of robotic-assisted endovascular surgery," *Expert Review of Medical Devices*, vol. 17, no. 9, pp. 919–927, 2020.

[2] J. Hasan, H. Asma, and K. Saibal, "Mitraclip: a novel percutaneous approach to mitral valve repair," *Journal of Zhejiang University-SCIENCE B (Biomedicine Biotechnology)*, vol. 12,(8):633-637, 2011.

[3] A. Mousa, S. Khoo, and M. Norton, "Robust control of tendon driven continuum robots," in *2018 15th International Workshop on Variable Structure Systems (VSS)*. IEEE, 2018, pp. 49–54.